Removal Characteristics of Gaseous Sulfur-Containing Compounds by Pulsed Corona Plasma

Nai-Qiang Yan,* Zan Qu, Jin-Ping Jia, Xiao-Peng Wang, and Dan Wu

School of Environmental Science and Engineering, Shanghai Jiao Tong University, 800 Dongchuan Road, Shanghai 200240, People's Republic of China

Pulsed corona plasma was employed to treat the gases containing hydrogen sulfide, methyl mercaptan (MM), and dimethyl sulfide (DMS), respectively. For the plasma oxidation only, the removal efficiencies of hydrogen sulfide, MM, and DMS were approximated to be 90%, 69%, and 52% when the discharge power was 5.6 W. But all the removal efficiencies were over 98% when an activated carbon fiber (ACF) filter was used downstream from the plasma reactor. In addition, the decomposition reaction mechanism was discussed and a competitive reaction kinetics model was proposed to describe the plasma decomposition reaction kinetics. The ACF filter appeared to be co-beneficial in the improvement of removal efficiency, reduction of energy consumption, and the abatement of ozone or other byproducts. The energy consumption was about 3 W·h/m^3 for hydrogen sulfide to obtain about 90% of the removal efficiency by plasma oxidation only, but it can be reduced below 1.2 W·h/m^3 in the present of the ACF filter.

Introduction

Odorous compounds emissions from various industrial processes, wastewater, or livestock production plants have been widely recognized as a problem. In many countries, complaints about odorous gases were the main cases among environmental pollution events.[1,2] Among the odorous substances, sulfur-containing compounds are the most representative pollutants with very low olfactory detection thresholds, such as hydrogen sulfide (H_2S), methyl mercaptan (MM), and dimethyl sulfide (DMS).[3,4] To treat these odorous gases, physical or chemical methods have been widely used, such as activated carbon adsorption, combustion, acid-alkali treatment, and so on.[5−8] However, the maintenance and operation costs of these methods were high and they easily caused secondary pollution.[9] Biological deodorization has been considered to be an attractive method; it displayed many advantages over the other typical methods to treat the low concentration odorous gases.[10,11] However, the adaptability of biotreatment to a higher concentration of odorous compounds or less water-soluble substances, such as organic sulfur-containing compounds, was relatively weak.[12]

Recently, the nonequilibrium plasma technology induced by pulsed corona discharge has attracted much attention to the treatment of hazardous air pollutants because of its potential advantages, such as the lower energy demand, lower capital investment, and the compacter apparatus.[13] Many studies have been carried out for the removal of sulfur dioxide and nitric oxide from coal-fired flue gases by means of the nonequilibrium plasma, and the pilot experiments have been performed in many countries.[13−15] In addition, pulsed corona discharge also showed high efficient to the abatement of the other gaseous pollutants, such as volatile organic compounds (VOCs) and mercury vapor.[16,17,19]

The decomposition of odorous gases by corona discharge plasma has been involved in the previous studies.[18−21] Helfritch investigated the decomposition behavior of hydrogen sulfide by the negative pulsed discharge.[18] But his experiment was aimed at producing hydrogen from hydrogen sulfide in the H_2/H_2S gas mixture (fuel gases, no oxygen involved), and the concentration of hydrogen sulfide was high (up to 2%). Winands et al. have reported the industrial demonstration results for low concentration level odor emission control by pulsed corona plasma, and the energy consumption was about 2 W·h/m^3 to obtain 95% of H_2S removal efficiency when the inlet H_2S concentration in the odorous gas mixtures was about 10 ppm.[19] Further, it was predicted that 0.2−0.4 W·h/m^3 was sufficient to realize a satisfactory deodorization for the low concentration odorous industrial gases.[19] However, there is still a lack of the necessary information on the removal of a higher concentration of odorous gases by the pulse corona plasma, such as the effects of the target pollutant concentration, energy consumption, and gas composition.

In addition, ozone and other byproducts often present in the treated gases by the plasma oxidation process, and the slip of ozone in the treated gases has been mentioned.[19] Different from the utilization of plasma oxidation in the hot flue gases condition, the plasma decomposition of odorous gases or VOCs often operated at around the ambient temperature, and the produced ozone was very stable in this condition.[20] Generally, the electric power consumption to produce the discharge plasma was larger for the treatment of the higher concentration odorous gases, and the produced ozone concentration was also higher in this case. The contribution of ozone to the decomposition of the target pollutant was very slight by the gas-phase reaction. Therefore, how to reuse the produced ozone in the treated gas and eliminate the potential pollution by the sulfur-containing byproducts from the plasma process still remain to be investigated for the treatment of the higher concentration odorous gases.

In this paper, the positive pulsed corona discharge plasma was employed to treat the odorous gases with the concentration level from tens to hundreds of milligrams per cubed meter at room temperature. Meanwhile, activated carbon fiber (ACF) was preliminarily used downstream the plasma reactor to abate the emission of ozone and other byproducts. In addition, the decomposition reaction kinetics and the possible mechanism were involved in this study. The simulated odorous gases contained hydrogen sulfide, MM, and DMS, respectively.

Material and Methods

Systematic Setup. The schematic circuit diagram of the experimental system is shown in Figure 1. The simulated

* To whom correspondence should be addressed. Fax: 86-21-54742817. E-mail: nqyan@sjtu.edu.cn.

10.1021/ie060471f CCC: $33.50
Published on Web 08/18/2006

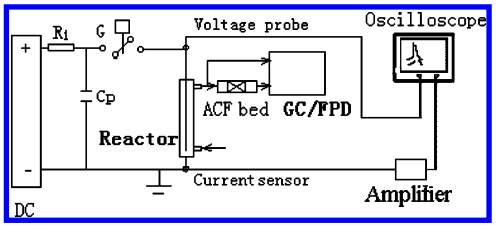

Figure 1. Schematic circuit diagram of the experimental system.

odorous gases used in the experiment were prepared by mixing the chemicals vapor with air. DMS was of analytical purity and purchased from Aldrich. Hydrogen sulfide or MM was prepared by the reaction of sodium sulfide or sodium methyl mercaptan (CH_3SNa) with sulfuric acid solution, and then the generated gases were dried with concentrated phosphorus acid. The high concentration gases (about 50% with nitrogen balanced) of H_2S, MM, and DMS were stored in Teflon gas bags (3.8 L, Chemware), respectively. A peristaltic pump was used to feed the high concentration H_2S, MM, or DMS gases to the air stream to prepare the diluted odorous gas with various concentrations. The prepared gases flowed through the discharge plasma reactor and then got across the ACF filter. The ACF was produced by Anshan ACF Plant (China); it was a polyacrylonitrile base fiber with about 1500 m^2/g of BET surface area. About 2.0 g of ACF was packed in a glass tube with the diameter of 30 mm, and the packed thickness was about 30 mm. All the experiments were performed at room temperature (296 ± 2 K) and 1 atm. The humidity of air was adjusted by water-bubbling, and the water vapor concentration in air was kept at about 1.5% if it was not stated clearly.

Power Supply and Discharge Reactor. The schematic circuit of the pulsed voltage supply consisted of the high direct current (DC) voltage supply, the storage capacitor, Cp, and the rotating spark gap switch. The output voltage from the DC source was positive and ranged from 0 to 70 kV, and the storage capacitor was charged by the DC source. The high voltage or the stored electric energy upon Cp was quickly delivered into the reactor when the spark gap switch was turned on, and the discharge occurred at the same time. The discharge frequency was controlled by adjusting the rotating speed of the spark switch, which was set at 85 Hz in this study. The configuration of the discharge plasma reactor used in this experiment was wire-tube type. The grounded electrode was a stainless steel tube with 57 mm in the inner diameter and 1200 mm in the length. The discharge electrode was a stainless steel wire with the diameter of 1 mm. The simulated odorous gas passed through the reactor from inlet and outlet ports, which were located on the two ends of the reactor, respectively.

The pulsed discharge parameters were measured with a digital phosphor oscilloscope (TektronixTD S5052), a high-voltage probe (Tek, P6015A), and an AC/DC current probe with an amplier (Tek, TCPA300). The discharge energy of every pulse can be calculated and displayed synchronously from the pulsed voltage and currency waveforms with the extension function of the oscilloscope.

The typical waveforms of the pulsed discharge voltage, currency, and power upon the reactor are shown in Figure 2. It was observed that the rising time of the pulsed voltage was very sharp, and it was around 50 ns. In addition, the discharge power in the reactor, P_w, can be calculated with eq 1.

$$P_w = fW \tag{1}$$

where f is discharge frequency in Hz and W is the discharge energy for a single pulse in J/pulse.

Analytical Methods and Accuracy. The concentration of the sulfur-containing compounds in the gases was measured by a gas chromatograph (GC-14B, Shimadzu Corp.) with a flame photometric detector (FPD-14, Shimadzu Corp.). The capillary column (DB-5) with the size of 30 m × 0.25 mm × 0.25 μm was used in the analysis. The carrier gas was nitrogen, and the flux was 1.0 mL/min. The column temperature was around 30−100 °C. GC-MS (QP2010NC, Angilent Corp.) was used to analyze the decomposition products from the pollutants. Sulfur dioxide and ozone concentration in the gases were measured with the detector tubes (Beijing Municipal Institute of Labour Protection).

The uncertainty for the measurement of the concentration of hydrogen sulfide, MM, and DMS was within ±2 mg/m^3, respectively. Every datum used for the calculation of removal efficiency was the average of at least three repeats. The accuracy of the flow rate was within ±0.05 m^3/h. The fluctuation for the discharge power measurement was less than 5%. Therefore, the relative error for the removal efficiency calculation was less than 5%, and it was estimated to be about 10% for the kinetics parameter evaluation.

Result and Discussion

Effect of the Discharge Power on the Removal of H_2S, MM, and DMS. The effect of the discharge power, P_w, on the removal efficiency of hydrogen sulfide, MM, and DMS is illustrated in Figure 3, in which the discharge power was adjusted by changing the applied voltage. The gas residence time was 5.1 s, and the inlet concentrations of hydrogen sulfide and MM in the gas were about 120 mg/m^3, respectively. The inlet concentration of DMS was about 110 mg/m^3.

It was obvious that the removal efficiency went up with the increase of voltage peak when V_D was above the onset discharge voltage, which was about 20 kV for the reactor used in this study. When V_D was 30 kV, the discharge power was about 0.95 W, and the density of radicals and other reactive species produced by the pulsed discharge was low. The removal efficiencies were only about 45% and 31% for hydrogen sulfide and MM. When the discharge power was 9 W at about 54 kV of the applied voltage, the discharge in the reactor became rather strong, which provided an effective oxidation circumstance to the decomposition of odorous compounds. Hereby, η of hydrogen sulfide and MM reached 97% and 82%, respectively. As for DMS, it appeared to be more difficult to be removed compared with hydrogen sulfide and MM. When P_w was 9 W, the removal efficiency was about 68%. The removal efficiencies of hydrogen sulfide, MM, and DMS were approximated to be 90%, 69%, and 52% when the discharge power was 5.6 W.

Effect of Gas Residence Time. The gas residence time in the reactor was determined by the gas flow rate (Q) through the reactor, and the shorter residence time means the shorter reaction time for the decomposition of odorous pollutants. The effect of gas residence time on the removal efficiency is shown in Figure 4. It was obvious that the removal efficiency increased as the gas residence time was prolonged when the discharge condition was given. The removal efficiencies of hydrogen sulfide and MM were about 96% and 82% when the residence time was 5.1 s. The efficiencies dropped below 80% and 60% if the residence time was about 1.8 s. The similar tendency between the removal efficiency and the residence time was observed with respect to DMS. The η values were about 82% and 46% when the gas residence times were 10.2 and 1.8 s, respectively.

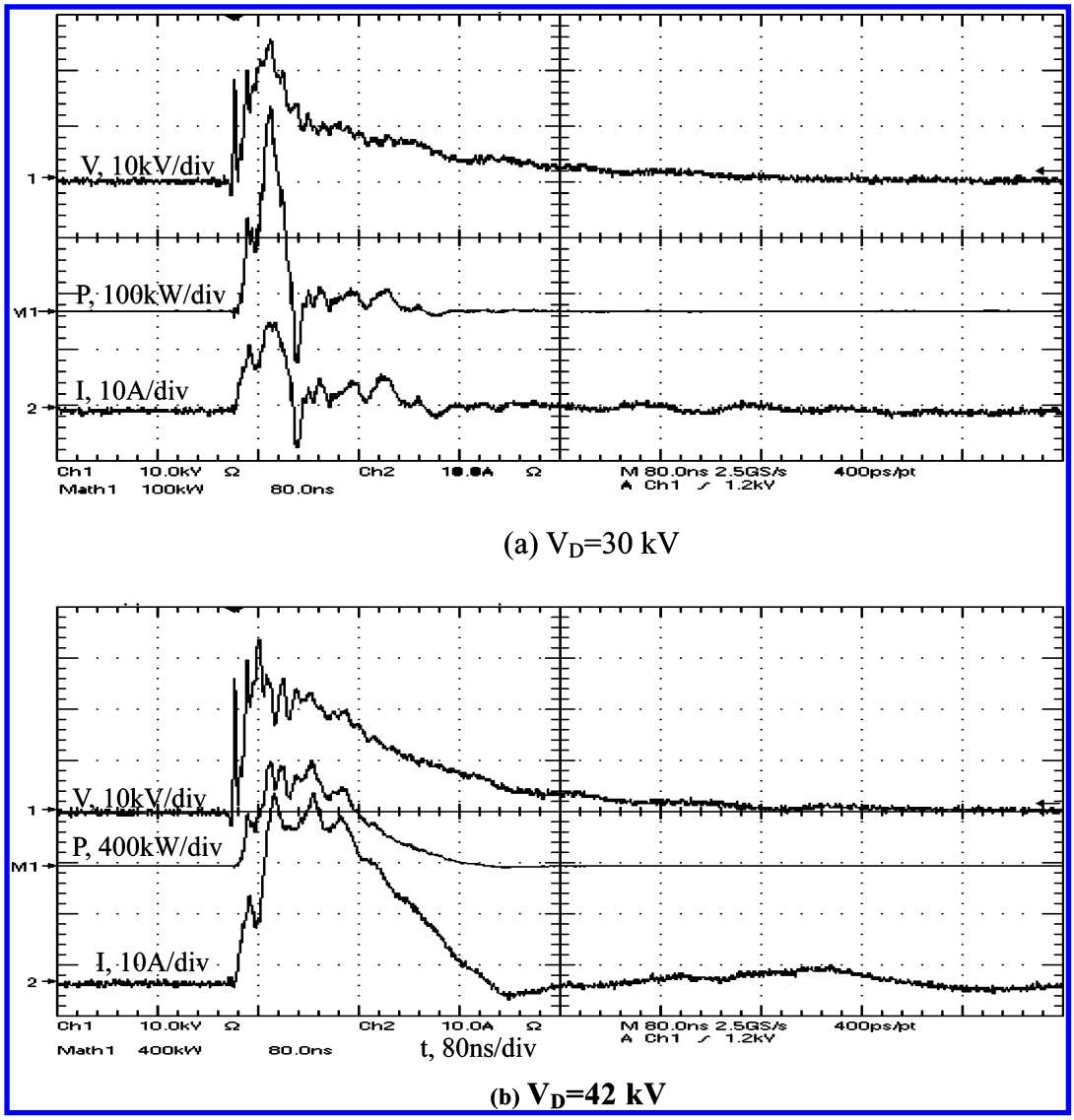

Figure 2. Pulse voltage, discharge currency, and power waveforms at different applied voltages. (a) V_D = 30 kV, discharge frequency 85 Hz, and (b) V_D = 42 kV, discharge frequency 85 Hz. The structure of the reactor is as follows: wire-tube type with the inner diameter of 57 mm and 1200 mm in the length. V_D denotes the voltage upon the storage capacitor, which is defined as the applied voltage, the voltage in the context.

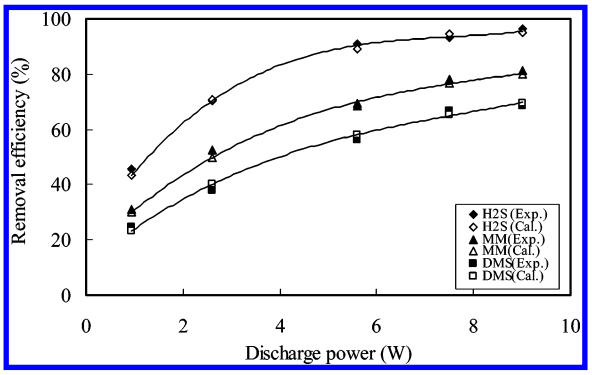

Figure 3. Effect of the discharge power on the removal efficiency of H_2S, MM, and DMS. Exp. means the experimental data; Cal. denotes the calculated data by eq 12. The inlet concentrations, C_i, of hydrogen sulfide, MM, and DMS were about 120 mg/m^3, 120 mg/m^3, and 110 mg/m^3, respectively. The gas residence time was 5.1 s.

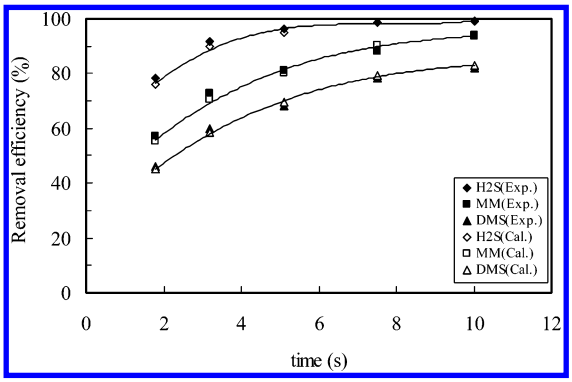

Figure 4. Removal efficiency of hydrogen sulfide, MM, and DMS vs gas residence time. Exp. means the experimental data; Cal. denotes the calculated data by eq 12. The inlet concentrations, C_i, of hydrogen sulfide, MM, and DMS were 120 mg/m^3, 120 mg/m^3, and 110 mg/m^3, respectively. The discharge power was 9 W.

Effect of the Inlet Concentration of Odorous Compounds. The effect of the inlet concentration of hydrogen sulfide, MM, and DMS on the removal efficiencies is shown in Figure 5, in which the discharge power was 9 W and the gas residence time was about 5 s. It was obvious that the removal efficiency decreased as the inlet concentrations rose. When the inlet concentration was about 70 mg/m^3 for the three compounds, the removal efficiencies were over 97%, 85%, and 76%, respectively. However, all the removal efficiencies dropped below 70% when the inlet concentration went up to 500 mg/

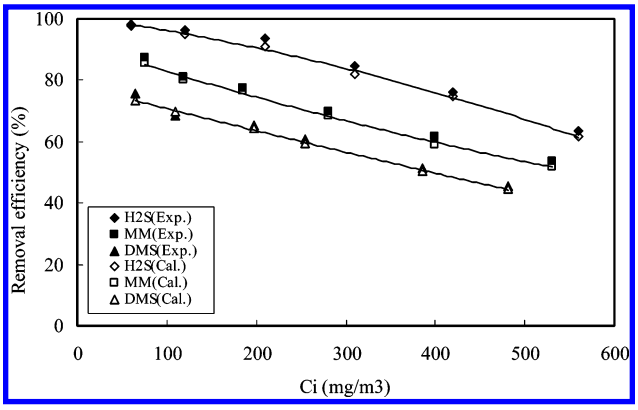

Figure 5. Removal efficiency of hydrogen sulfide, MM, and DMS vs the their inlet concentrations. Exp. means the experimental data; Cal. denotes the calculated data by eq 12. The discharge power was 9 W. The gas residence time was 5.1 s.

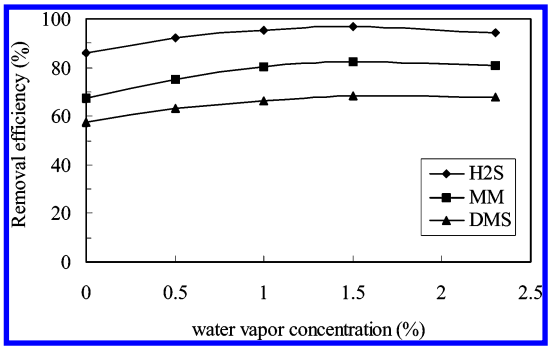

Figure 6. Removal efficiency of hydrogen sulfide, MM, and DMS vs water vapor concentration in the gases. The inlet concentrations, C_i, of hydrogen sulfide, MM, and DMS were about 120 mg/m^3, 120 mg/m^3, and 110 mg/m^3, respectively. The discharge power was 9.0 W, and the gas residence time was 5.1 s.

m^3. It could be explained that the densities of radicals and reactive species approximately remained constant at the given discharge condition. The higher inlet concentration of the pollutants would need more radicals and other reactive species, which might become insufficient for the decomposition of odorous molecules. Therefore, the discharge plasma appeared to be more efficient for the treatment of the low concentration odorous gases.

Effect of Water Vapor Concentration. The effect of water vapor concentration on the removal efficiency of H_2S, MM, and DMS is shown in Figure 6, in which the discharge power was 9 W. The removal efficiency of every compound went up when gas humidity increased from 0 to 1%, but too higher humidity still showed inhibition to the removal of every compound. Water vapor can be dissociated to the reactive OH radical by the impact of energetic electrons, which was helpful to the oxidation of the gaseous pollutants. However, the water vapor molecule was also strongly electronegative, and a high concentration of water vapor would inhibit the development of the discharge streamer and reduce the plasma volume in the reactor, which resulted in the decrease of the removal efficiency.

Decomposition Products and Discussion on the Reaction Mechanism. The main decomposition products of hydrogen sulfide, MM, and DMS under discharge plasma were analyzed. For H_2S decomposition, the main product was sulfur dioxide. Also, a small amount of elemental sulfur was observed to deposit on the surface of the discharge electrode. But the elemental sulfur would not be accumulated excessively due to the further oxidation by the discharge. Because the olfactory detection threshold of SO_2 was higher and the odorous intensity of SO_2 was weaker than that of H_2S at the same concentration, and it was regarded as an effective method to convert H_2S to SO_2. Also, sulfur trioxide was also supposed to be the product of H_2S decomposition, but the measurement method in this study was not sensitive to it. Ozone was also an important byproduct in the treated gas. The concentration of ozone increased with the rise of the discharge power.

To detect the decomposition products and the interim products of MM and DMS, a higher inlet concentration (about 1%) of pollutants and lower discharge power were used. The GC-MS spectrum of the treated gas containing MM is shown in Figure 7a. It was found that dimethyl disulfide (DMDS) was the main interim product for MM when the discharge plasma was not very strong. Also, small amounts of DMS, dimethyl sulfoxide and other oxygen-containing hydrocarbons (such as methanol and organic acid) were also found. As for DMS, DMDS, dimethyl sulfoxide, and other oxidized hydrocarbons were also found from Figure 7b. In addition, dimethyl sulfone was supposed to be the byproduct of MM or DMS, but it was not detected by the GC-MS technique, which maybe resulted from its low volatility and strong polarity. The above byproducts can be significantly reduced as the discharge power increased, and sulfur dioxide and carbon dioxide were still the main products of MM and DMS.

The plasma oxidation of H_2S, MM, and DMS can be described as follows. First, the radicals and other active species, A* (such as O•, OH•, etc.), were formed by energized electron collisions with oxygen or water vapor in the gas.[21−23] Then, A* reacted with pollutant molecules and decomposed them (effective reactions). At the same time, A* can react with other species to be consumed (unwanted reactions), and the main decay reactions for O and OH are described with eqs 2−4.[22−24] The decay reactions of O and OH radicals were competitive with the reactions to decompose the pollutants.

$$O + O_2 + M \rightarrow O_3 + M \quad (2)$$

$$OH + O + M \rightarrow HO_2 + M \quad (3)$$

$$OH + OH + M \rightarrow H_2O_2 + M \quad (4)$$

The decomposition reaction approaches of hydrogen sulfide could be deduced according to the decomposition products. The H_2S molecule was first oxidized to some interim species (such as HS• and S•) by the produced radicals or other active species; then, the interim species were oxidized partially to elemental sulfur or deeply oxidized to sulfur dioxide or sulfur trioxide.

The decomposition approaches for MM and DMS have not been understood clearly, but any speculations can be deduced from their interim products. For MM, the lower bond energy of S−H (bonding energy, 347.3 kJ/mol) in its molecular structure easily caused the disassociation reactions or the hydrogen abstraction reactions in the presence of other radicals and other active species, so CH_3S• and CH_3• were the primary interim radicals in this process.[25] CH_3S• and CH_3• can be further oxidized when the radicals and other active species were abundant, but a small amount of $CH_3-S-S-CH_3$ (DMDS) and $CHSCH_3$ (DMS) can be produced by the recombination reaction, which depended on the concentration of CH_3S•, CH_3•, and A*. Similarly, the decomposition of DMS also went through a series of processes, which were involved in the disassociation,

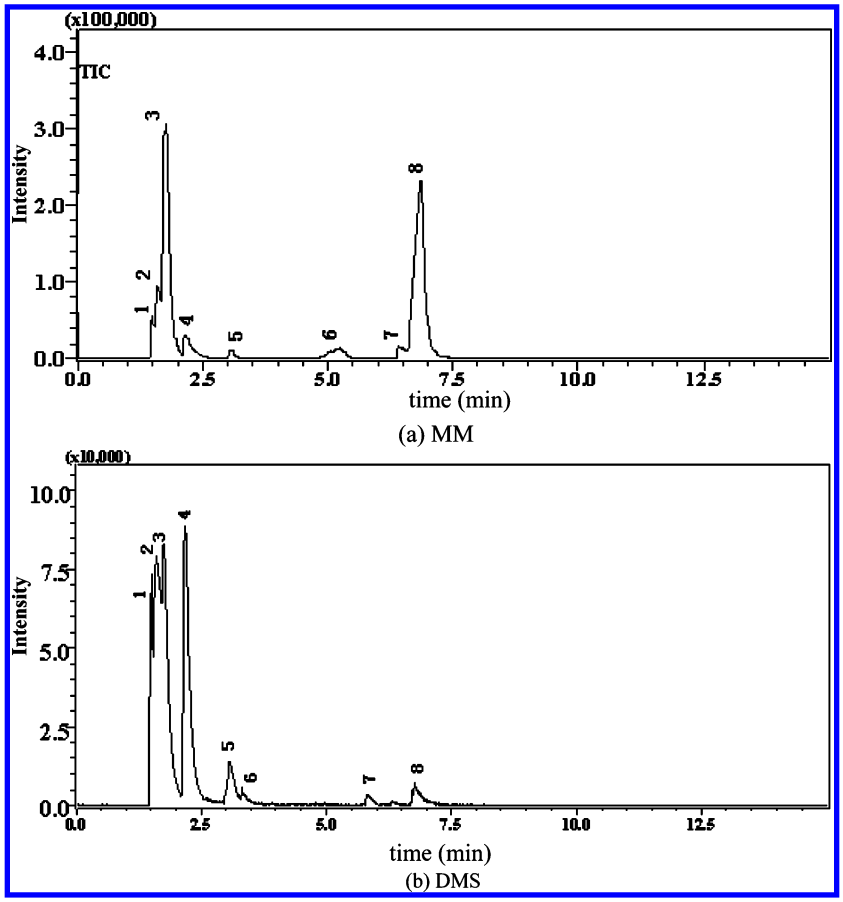

Figure 7. GC-MS spectrums of the treated gases containing MM and DMS. The inlet concentrations of MM and DMS were about 1%, respectively. The discharge power was 2.5 W. The treatment time was about 20 s at 296 ± 2 K and 760 Torr. The detected components and their reliabilities (in parentheses) in the gases were as follows. (a) 1, CH_3OH (85%); 2, SO_2 (overlapped with CO_2; 90%); 3, CH_3SH (100%); 4, CH_3SCH_3 (100%); 5, CH_3COOH (80%); 6, CH_3CH_2COOH (70%); 7, CH_3SOCH_3 (70%); and 8, CH_3SSCH_3 (100%). (b) 1, CH_3OH (85%); 2, SO_2 (overlapped with CO_2; 90%); 3, CH_3CH_2OH (80%); 4, CH_3SCH_3 (100%); 5, CH_3COOH (80%); 6, $CH_3CHOHCH_2OH$ (70%); 7, CH_3SOCH_3 (70%); and 8, CH_3SSCH_3 (100%).

recombination, oxidation, and so forth. The main presumed reactions were expressed as follows.

$$CH_3SH + A^* \rightarrow CH_3OH, CH_3S\bullet, CH_3\bullet, \text{etc.} + A^* \rightarrow SO_2, CO_2, H_2O, \text{etc.} \quad (5)$$

$$CH_3SCH_3 + A^* \rightarrow CH_3OH, CH_3SCH_2\bullet, CH_3S\bullet, CH_3\bullet, \text{etc.} + A^* \rightarrow SO_2, CO_2, H_2O, \text{etc.} \quad (6)$$

$$CH_3S\bullet + CH_3S\bullet \rightarrow CH_3SSCH_3 \quad (7)$$

$$CH_3S\bullet + CH_3\bullet \rightarrow CH_3SCH_3 \quad (8)$$

$$CH_3SCH_3 + O\bullet \rightarrow CH_3{-}SO{-}CH_3, CH_3{-}SO_2{-}CH_3 \quad (9)$$

Determination of the Plasma Decomposition Kinetics. The plasma oxidation reaction kinetics for the decomposition of odorous substances has not been clearly understood yet. Helfritch[18] has studied the decomposition kinetics of H_2S in the $H_2{-}H_2S$ gas mixture, and the decomposition rate was observed to be positive proportional to the discharge power in the same reactor. Young et al.[23] also assumed that the plasma oxidation of hydrocarbon conformed to the first-order mode with respect to the discharge power, which can be expressed as

$$dC/dt = -k_d P_w/Q \quad \text{or} \quad \ln(C_o/C_i) = k_d P_w/Q \quad (10)$$

where C_i and C_o are the inlet and outlet concentrations of the pollutant, respectively. Q was the flow rate of the gas. P_w is the discharge power. k_d is the decomposition reaction rate constant.

According to eq 10, C_o/C_i or the removal efficiency, $(1 - C_o/C_i) \times 100\%$, should be a constant when P_w/Q was given. However, it was observed according to our study that eq 10 was only applicable to the case for the treatment of low concentration gas. According to this study, when the inlet concentration of H_2S (or MM, DMS) ranged from tens to hundreds mg/m^3, the deviation was very significant if eq 10 was used to describe the decomposition kinetics of H_2S, MM, and DMS, as can be observed from Figure 5.

The difference between the tested decomposition kinetics and the expected first-order mode (eq 10) maybe resulted from the complexity and nonselectivity of the reactions involved in the radicals and active species and the competition between the decomposition reaction of odorous compounds and the decay reaction of radicals resulted in the above deviation. According to the observed decomposition characteristic, a competitive model was put forward to describe the decomposition reaction kinetics of pollutants by discharge plasma. Equation 11 was proposed by us to describe the removal kinetics of H_2S, MM, and DMS.

$$dC/dt = k_d {P_w}^m Q^n \frac{C}{C + \beta} \quad (11)$$

in which k_d is the decomposition reaction rate constant and Q is gas flow rate. C is the concentration of the pollutant. m, n,

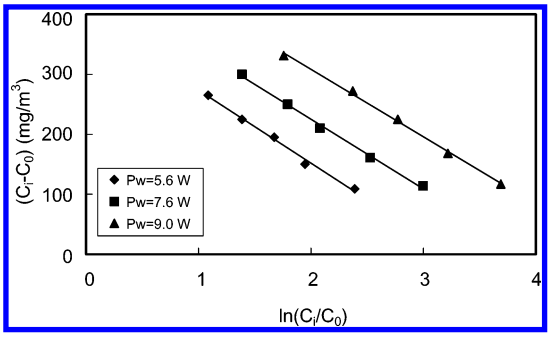

Figure 8. Relationship between $\ln(C_i/C_o)$ and $C_i - C_o$ for H_2S decomposition. The inlet concentration of hydrogen sulfide ranged from 50 to 550 mg/m^3. The gas residence time was 5.1 s.

and β are the coefficients that will be determined experimentally. Equation 11 can be integrated and described as eq 12 when the inlet and outlet concentration of the pollutant are involved.

$$C_i - C_o = -\beta \ln(C_i/C_o) + V_R k_d P_w{}^m Q^{n-1} \qquad (12)$$

where C_i and C_o are the inlet and outlet concentrations of the pollutant, respectively. V_R is the volume of the discharge plasma reactor. To estimate the value of the main parameters, the units of the variables were set as follows: V_R, m^3; C_i or C_o, mg/m^3; P_w, W; Q, m^3/h; m or n, dimensionless; and the group of $P_w{}^m Q^{n-1}$, dimensionless. Therefore, the units of β and k_d were mg/m^3 and mg/m^6, respectively.

According to eq 12, β and $k_d P_w{}^m Q^{n-1}$ can be graphically determined from the relation $\ln(C_i/C_o)$ and $C_i - C_o$ when different C_o was employed. If $C_i - C_o$ was linear to $\ln(C_i/C_o)$, then the slope of the line would be the value of $-\beta$. The relationship of $(C_i - C_o)$ and $\ln(C_i/C_o)$ for H_2S decomposition is shown in Figure 8, in which Q was 2.2 m^3/h at various discharge powers.

It was obvious that the curves for the different discharges were nearly parallel to one another, and the correlative coefficients, R, for each curve were all around 0.99. This indicated that eq 12 or 11 was suitable to describe the decomposition kinetics of hydrogen sulfide. β was obtained from the slopes of the curves, and it remained a constant at the different applied voltages, which was about 95 ± 10 mg/m^3 for hydrogen sulfide. However, the intercepts of each curve, $k_d P_w{}^m Q^{n-1}$, increased with the rise of the discharge power, and m was estimated from the relationship between $k_d P_w{}^m Q^{n-1}$ and P_w; it was about 0.62 ± 0.05.

In addition, the dependence of $k_d P_w{}^m Q^{n-1}$ on the gas flow rate, Q, was investigated as Q ranged from 0.6 m^3/h to 2.8 m^3/h. n can be obtained from the dependence of $k_d P_w{}^m Q^{n-1}$ on Q, and it was around -0.38 ± 0.03. Therefore, k_d can be calculated as 6.1 ($\pm$0.3) $\times$ 10^4 mg/m.[6]

Similarly, the decomposition kinetics for MM and DMS can also be described well with eq 11 or 12. The main kinetics parameters were listed in Table 1. The β values for MM or DMS were larger than that for hydrogen sulfide, which indicated that the utilization efficiency of the active species was lower for the decomposition of MM or DMS, especially for DMS. In addition, the k_d values for MM or DMS were slight lower than that for H_2S. In addition, the calculated removal efficiencies for H_2S, MM and DMS by eq 12 and Table 1 are also shown in Figures 3−5, which were well applicable in most of the cases.

Integrated System of Plasma Oxidation with the Downstream ACF Filter. According to the above analysis results, the removal efficiency of MM and DMS by discharge plasma was not high enough to meet the environmental purpose when the inlet concentration of these compounds was about 50 mg/m^3 or higher, and the demanded discharge power was rather high. Meanwhile, the emission of the sulfur-containing byproducts and ozone was another issue to be considered. The formation of ozone (produced through reaction 2) was almost inevitable in the discharge environment with oxygen. However, the gas-phase reaction rate of ozone and the target compounds was too slow to have any significant contribution to the removal efficiency in the employed gas retention time (several seconds).[20]

Table 1. Kinetics Parameters for the Decomposition of H_2S, MM, and DMS[a]

	H_2S	MM	DMS
β (mg/m^3)	95 ± 10	170 ± 10	220 ± 10
k_d ($\times 10^4$ mg/m^6)	6.1 ± 0.3	5.7 ± 0.3	5.2 ± 0.3
m	0.61 ± 0.2	0.61 ± 0.2	0.61 ± 0.2
n	0.38 ± 0.2	0.38 ± 0.2	0.38 ± 0.2

[a] k_d is defined as the decomposition reaction rate constant, Q was the gas flow rate, and P_W was the discharge power. The inlet concentration of hydrogen sulfide, MM, and DMS ranged from 50 to 550 mg/m^3, respectively.

Table 2. Concentration of the Odorous Compounds and Byproducts in the Outlet Gases with/without the Downstream ACF Filter[a]

		without the downstream ACF filter (mg/m^3)				with the downstream ACF filter (mg/m^3)			
compound	power, P_w (W)	C_o	$[O_3]$	$[SO_2]$	DMDS	C_o	$[O_3]$	$[SO_2]$	DMDS
H_2S	0	118	0	0	0	106	0	0	0
	2.5	38	31	51		<3	4	<2	
	5.6	15	48	66		<1	5	<2	
MM	0	115	0	0	0	104	0	0	0
	5.6	42	43	37	D	<1	5	<2	N/D
DMS	0	112	0	0	0	94	0	0	0
	5.6	58	39	28	D	<1	5	<2	N/D

[a] The gas flow rate was about 2.2 m^3/h. About 2.0 g of ACF was packed in a glass tube with the diameter of 30 mm, and the packed thickness was about 30 mm. D means DMDS was detectable by GC-MS measurement, but N/D means it was not detectable.

Untreated ACF Filter. To overcome these problems, a compact filter consisting of ACF was tentatively used downstream the discharge reactor. Compared with the granular activated carbon, the ACF filter was light and had a high specific surface area and low gas resistance. Therefore, the application of ACF material in environmental technology has been paid more attention recently.[26,27]

The contribution of the ACF filter to the removal of the original pollutants, byproducts, and ozone is listed in Table 2. It can be seen that the ACF filter can remove H_2S, MM, and DMS by adsorption when the plasma reactor was out of operation ($P_w = 0$), but the adsorption ability decreased quickly as the accumulation of the adsorbed compounds. When the adsorption time was about 3 h, the removal efficiency of H_2S, MM, and DMS decreased to 15% by the adsorption of the ACF filter. When the plasma reactor worked ($P_w = 5.6$ W), the target pollutants were almost completely removed by the combination of discharge plasma and the downstream ACF filter, and the removal efficiency remained over 98% for at least 5 h. Meanwhile, ozone, SO_2, and DMDS can be removed simultaneously, and the ozone concentration in the effluent gas was less 5 mg/m^3 with about 90% of removal efficiency. SO_2 and DMDS were also abated dramatically.

According to the mass balance of the original pollutants, the contribution of the ACF filter to the removal of H_2S, MM, and DMS appeared to have multiple effects, not merely by adsorption, and the chemical reaction was supposed to be concurrent on the ACF surface. The adsorbed ozone and other long-life

Table 3. Concentration of the MM and Byproducts in the Outlet Gases with the Downstream Pretreated ACF Filter[a]

		with the downstream ACF filter (mg/m^3)			
sorbent	power, P_w (W)	C_o	[O_3]	[SO_2]	DMDS
untreated, ACF	0	104	0	0	0
	2.5	13	4	2	N/D
KI/ACF	0	108	0	0	0
	2.5	6	N/D	N/D	N/D
Mn /ACF	0	112	0	0	0
	2.5	5	<1	<1	N/D
Fe/ACF	0	109	0	0	0
	2.5	11	<1	<1	N/D

[a] The gas flow rate was about 2.2 m^3/h. About 2.0 g of ACF (virgin or pretreated) was packed in a glass tube with the diameter of 30 mm, and the packed thickness was about 30 mm. N/D meant it was not detectable by GC-MS measurement.

reactive species, such as H_2O_2 (produced from the reaction 4) and negative oxygen ions, were supposed to react with odorous compounds on the ACF surface. Though the gas-phase reaction between H_2S (or MM, DMS) and ozone was slow, the adsorbed states of these substances would react with each other more easily. Therefore, these adsorbed pollutant compounds were supposed to be oxidized quickly and fully in the presence of ozone and other long-life reactive species. The main reaction approaches are illustrated as eqs 13−15.

$$H_2S^{(a)}\ (\text{or MM, DMS}) + O_3^{(a)}\ (\text{or } O^-) \rightarrow SO_2,\ SO_3,\ \text{DMSO, etc.} \quad (13)$$

$$SO_2^{(a)} + O_3^{(a)}\ (\text{or } O^-) \rightarrow SO_3 \quad (14)$$

$$\text{DMDS}^{(a)} + O_3^{(a)}\ (\text{or } O^-) \rightarrow \text{DMDSO} \quad (15)$$

where the subscript "(a)" refers to the adsorbed species on ACF surface and DMDSO represents dimethyl disulfone. All the deep oxidized products on ACF were well-soluble in water, and the filter can be easily regenerated by water washing.

On the grounds of the above result, it was obvious that the utilization of the ACF filter downstream from the plasma reactor was co-beneficial, which can not only increase the removal efficiency of the original pollutants but also abate the emission of ozone and other hazardous byproducts.

Pretreated ACF Filter. As seen from Table 2, though the integrated ACF filter can remove the target pollutants and surfur-containing byproducts effectively, it cannot remove ozone completely (only about 80−90%). To promote the removal of ozone by the ACF filter, solutions with potassium iodide (KI), iron(III) nitrate, and manganese nitrate were used to impregnate ACF material, respectively. The impregnation amount of potassium iodide on ACF was about 1 wt %, and the impregnated ACF was dried at 373 K for 2−3 h. The impregnation amount of iron nitrate or manganese nitrate on ACF was also about 1 wt %, and the impregnated ACF was dried at 373 K for 2 h and followed by calcination at 653 K for 2 h to convert the nitrates to oxides.

The ACF impregnated with different reagents was used together with the plasma reactor to treat the gas containing MM, and the results are listed in Table 3. When the plasma reactor did not work, the removal efficiency of MM by adsorption of the impregnated ACF dropped slightly compared with that of the virgin ACF. However, all the impregnated ACF displayed good performance to remove ozone produced by discharge plasma, in which KI impregnated ACF appeared to be the best and nearly 100% of ozone was removed. The slip of ozone from the other two impregnated ACF filters was also very low. Meanwhile, the removal efficiency of MM in the KI/ACF filter and Mn/ACF filter increased slightly compared with that of the virgin ACF filter, and the overall removal efficiency by the integrated plasma oxidation with the impregnated ACF filter was about 95% when the discharge power was about 2.5 W. The Mn/ACF filter can also improve the removal efficiency of DMS downstream from the plasma reactor. However, it was observed that the KI/ACF filter was less effective to remove DMS than the virgin ACF, which indicated that KI or I_2 on the ACF have an insignificant effect to the oxidation of DMS.

In addition, the lifetimes of the ACF impregnated with KI and Mn were preliminarily tested for the removal of MM, in which the test conditions were the same as that in Table 3 (P_w = 2.5 W). For KI/ACF, the removal efficiency of MM remained over 95% for about 8 h. Thereafter, it gradually decreased, and the removal efficiency was about 85% when the accumulated operation time was 11.5 h, and ozone slip from the filter became significant at the same time. The similar tendency was observed for Mn/ACF, and the operation time lasted about 9 and 15 h to obtain over 95% and 85% of MM removal efficiencies, respectively. The reason for the decrease of KI/ACF and Mn/ACF to remove MM and ozone can be attributed to the coverage of the ACF surface by low-volatile compounds, for example, SO_3, H_2SO_4, DMSO, and so forth.

When the removal efficiency of MM was lower than 85%, the ACF filter was regenerated by water washing. After it was dried (at 80 °C for 2−3 h), the performance of the regenerated ACF filter was tested again. It was found that the Mn/ACF filter was almost completely recovered their original capacity for MM removal. However, the regenerated KI/ACF filter lost most of the impregnated KI, and its performance for MM and ozone removal was just close to that for the virgin ACF filter.

The promotion of KI and Mn oxide on ACF can be explained as follows. KI on ACF with moisture can react with ozone and other oxidative species to form iodine (I_2), which was helpful to capture ozone or other oxidative species from gas besides ACF adsorption. The produced iodine was also an oxidant, and then it can react with MM and other byproducts; iodine was reduced to iodide again (e.g., $2MM + I_2 \rightarrow DMDS + 2I^- + 2H^+$). Thus, KI acted as a catalyst in the process. Similarly, Mn and iron oxides have been demonstrated to be able to catalyze the decomposition of ozone, and an oxygen radical was produced as the short-life interim species, which can react with the target pollutant and byproducts quickly.[28,29] Because the impregnated ACF had to be washed frequently to remove the final products (e.g., H_2SO_4 and DMSO), the loss of KI would be significant. Therefore, the impregnation of Mn oxide or iron oxide on ACF would be preferred. In addition, the optimization of the combination between the discharge plasma and the pretreated ACF filter maybe resulted in higher removal efficiency at the lower discharge power, which deserved a further study.

Evaluation of the Energy Consumption and Technology Implication. The energy consumption was an important parameter for a pollution control technology. According to the above experimental result, the demanded discharge energy for H_2S, MM, and DMS was much different at a given removal efficiency. When the inlet concentration of H_2S was about 80 mg/m^3, the lowest energy consumption was about 3.0 W·h/m^3 to obtain about 90% of the removal efficiency, which indicated that about 3 kW·h of electric energy was consumed to treat 1000 m^3 of the odorous gas. Similarly, it was about 4.0

W·h/m^3 to obtain about 80% of the removal efficiency for MM. However, the demanded energy was rather high for DMS removal; it was up to 12 W·h/m^3 to obtain 80% of the removal efficiency. The energy consumption for the treatment of such a concentration of sulfur-containing compounds appeared to be high if only by discharge plasma oxidation. However, the energy consumption can be reduced dramatically when the ACF filter was used downstream, and it was less than 1.2 W·h/m^3 for H_2S to reach to 98% of the removal efficiency from the result in Table 3. It was predicted that the energy consumption in the larger scale experiment could be further reduced by the optimization of the reactor structure, the discharge parameters, and the combination with the downstream ACF adsorption.

In conclusion, the integration of discharge plasma with the downstream ACF was a co-beneficial method, which can increase the removal efficiency of odorous compounds, reduce the energy consumption as well, and abate the re-emission of ozone and/or other byproducts.

Conclusion

To develop an economical and efficient method to treat the higher concentration odorous gases, plasma induced by pulsed corona discharge was investigated to treat odorous gases containing hydrogen sulfide, MM, and DMS. The main factors that influenced the removal efficiency of odorous compounds were investigated experimentally. The removal efficiencies of hydrogen sulfide, MM, and DMS were approximated to be 90%, 69%, and 52% when the discharge power was 5.6 W. Increasing the discharge power or the gas residence time would bring higher removal efficiency. The combination of discharge plasma with the ACF filter downstream can increase the removal efficiency of odorous compounds, abate the emission of ozone and other byproducts, and reduce the energy consumption as well.

In addition, the reaction kinetics for the decomposition was investigated, a competitive model was proposed to describe the decomposition reaction kinetics, and the main kinetics parameters were experimentally determined. The products from the decomposition of hydrogen sulfide, MM, and DMS were analyzed, and the reaction mechanism was discussed. The energy demand for H_2S removal was about 3 W·h/m^3 to obtain about 90% of the removal efficiency, but it was over 12 W·h/m^3 for the treatment of DMS. The energy consumption can be reduced to less than 1.2 W·h/m^3 for H_2S to reach to 95% of the removal efficiency when the ACF filter was employed at the same time. The combination of the discharge plasma with an ACF filter appeared to be a promising method for the treatment of the higher odorous gases.

Acknowledgment

This work was supported by NSFC (Project No. 20077017), and the authors are grateful to Dr. Li Longhai for the assistance on the measurement of discharge parameters.

Literature Cited

(1) Kaye, R. A relationship between odour complaints and modeling out. Presented at National workshop on odour measurement standardization, Aug 1997, Sydney.

(2) Frechen, F.; Koester, W. Odor emission capacity of wastewaters − standardization of measurement method and application. *Water Sci. Technol.* **1997**, *38*, 61.

(3) Kenson, R. Controlling odors. *Chem. Eng.* **1981**, 94.

(4) Nourbakhsh, K.; Norwood, H.; Yin, C.; Liao, C.; Ng, C. Vacuum ultraviolet photodissociation and photoionization studies of CH_3SCH_3 and CH_3S. *J. Chem. Phys.* **1991**, *95*, 5014.

(5) Durme, G.; McNamara, B.; McGihley, C. Bench-scale removal of odor and volatile organic compounds at a composting facility. *Res. J. Water Pollut. Control Fed.* **1992**, *64*, 19.

(6) Cullis, C. The Kinetics of Combustion of Gaseous, Sulphur Compounds. *Combust. Flame* **1972**, *18*, 225.

(7) Turk, A.; Sakalis, E.; Lessuck, J.; Karamitsos, H.; Rago, O. Ammonia injection enhances capacity of activated carbon for hydrogen sulfide and methyl mercaptan. *Environ. Sci. Technol.* **1989**, *23*, 1242.

(8) Ikeda, H.; Asaba, H.; Takeuchi, Y. Removal of H_2S, CH_3SH and $(CH_3)_3N$ from air by use of chemically treated activated carbon. *J. Chem. Eng. Jpn.* **1988**, *212*, 91.

(9) Chu, H.; Lee, W.; Horng, K.; Tseng, T. Catalytic incineration of $(CH_3)_2S$ and its mixture with CH_3SH over a Pt/Al_2O_3 catalyst. *J. Hazard. Mater.* **2001**, *B82*, 43.

(10) Ottengraf, S. Exhaust gas purification. *Biotechnology* **1986**, *8*, 425.

(11) Williams, T.; Miller, F. C. Odor control using biofilters. *Biocycle* **1992**, *10*, 72.

(12) Hirai, M.; Masatoshi, M.; Shoda, M. Removal kinetics of hydrogen sulfide, methanethiol and dimethyl sulfide by peat biofiltrarion. *J. Ferment. Bioeng.* **1990**, *70*, 334.

(13) Masuda, S.; Nakao, H. Control of NO x by positive and negative pulsed corona discharges. *Conference Records of the IEEE/IAS Annual Meeting*, Denver, 1986; p 1173.

(14) Yan, K.; Yamamoto, T.; Kanazawa, S.; Ohkubo, T.; Nomoto, Y.; Chang, J. Control of flow stabilized positive corona discharge modes and NO removal characteristics in dry air by CO_2 injections. *J. Electrost.* **1999**, *46*, 207.

(15) Chang, J. Recently Development of Plasma Pollution Control Technology: a critical Review. *Sci. Technol. Adv. Mater.* **2001**, 571.

(16) Sobacchi, M.; Saveliev, A.; Fridman, A.; Gutsol, A.; Kennedy, L. Experimental Assessment of Pulsed Corona Discharge for Treatment of VOC Emissions. *Plasma Chem. Plasma Process.* **2003**, *23*, 347.

(17) Oda, T. Non-thermal plasma processing for environmental protection: decomposition of dilute VOCs in air. *J. Electrost.* **2003**, *57*, 293−311

(18) Helfritch, D. Pulsed corona discharge for hydrogen sulfide decomposition. *IEEE Trans. 1nd. Appl.* **1993**, *29*, 882.

(19) Winands, H.; Yan, K.; Nair, S.; Pemen, G.; Heesch, B. Evaluation of corona plasma techniques for industrial applications: HPPS and DC/AC systems. *Plasma Processes Polym.* **2005**, *2*, 232.

(20) Oda, T; Takahashi, T.; Yamaji, K. TCE Decomposition by the Nonthermal Plasma Process Concerning Ozone Effect. *IEEE Trans. Ind. Appl.* **2004**, *40* (5), 1249.

(21) Young, S.; Chang, M.; Moo, H.; In-Sik, N. Decomposition of Volatile Organic Compounds and Nitric Oxide by Nonthermal Plasma Discharge Processes. *IEEE Trans. Plasma Sci.* **2002**, *30*, 408.

(22) Yan, N.; Wu, Z.; Tan, T. Modeling of formaldehyde destruction under pulsed discharge plasma. *J. Environ. Science Health, Part A* **2000**, *35*, 1951.

(23) Kulikovsky, A. Production of chemically active species in the air by a single positive streamer in a nonuniform field. *IEEE Trans. Plasma Sci.* **1997**, *25*, 439.

(24) Li, J.; Sun, W.; Pashaie, B.; Dhali, S. Streamer discharge simulation in flue gas. *IEEE Trans. Plasma Sci.* **1995**, *23*, 672.

(25) Tsai, C.; Lee, W.; Chen, C.; Liao, W. Decomposition of CH_3SH in a RF plasma reactor: reaction products and mechanisms. *Ind. Eng. Chem. Res.* **2001**, *40*, 2384.

(26) Katoh, H.; Kuniyoshi, I.; Hirai, M.; Shoda, M. Studies of the oxidation mechanism of sulfur containing gases on wet activated carbon fiber. *Appl. Catal., B* **1995**, *6*, 255.

(27) Feng, W.; Kwon, S.; Borguet, E.; Vidic, R. Adsorption of hydrogen sulfide onto activated carbon fibers: Effect of pore structure and surface chemistry. *Environ. Sci. Technol.* **2005**, *39*, 9744.

(28) Dhandapani, B.; Oyama, S. Gas phase ozone decomposition catalysts. *Appl. Catal., B* **1997**, *11*, 129.

(29) Einaga, H.; Futamura, S. Comparative study on the catalytic activities of alumina-supported metal oxides for oxidation of benzene and cyclohexane with ozone. *React. Kinet. Catal. Lett.* **2004**, *81*, 121.

Received for review April 16, 2006
Revised manuscript received June 25, 2006
Accepted July 21, 2006

IE060471F